

RSC Advances



This is an *Accepted Manuscript*, which has been through the Royal Society of Chemistry peer review process and has been accepted for publication.

Accepted Manuscripts are published online shortly after acceptance, before technical editing, formatting and proof reading. Using this free service, authors can make their results available to the community, in citable form, before we publish the edited article. This *Accepted Manuscript* will be replaced by the edited, formatted and paginated article as soon as this is available.

You can find more information about *Accepted Manuscripts* in the [Information for Authors](#).

Please note that technical editing may introduce minor changes to the text and/or graphics, which may alter content. The journal's standard [Terms & Conditions](#) and the [Ethical guidelines](#) still apply. In no event shall the Royal Society of Chemistry be held responsible for any errors or omissions in this *Accepted Manuscript* or any consequences arising from the use of any information it contains.

Isoindigo Derivatives for Application in *p*-Type Dye Sensitized Solar Cells

*Dorine Ameline,^a Stéphane Diring,^a Yoann Farre,^a Yann Pellegrin,^a Gaia Naponiello,^b Errol Blart,^a Benoît Charrier,^a Danilo Dini,^b Denis Jacquemin,^{*ac} Fabrice Odobel^{*a}*

^a*Université LUNAM, Université de Nantes, CNRS, Chimie et Interdisciplinarité: Synthèse, Analyse, Modélisation (CEISAM), UMR 6230, 2 rue de la Houssinière, 44322 Nantes cedex 3, France. E-mail: Fabrice.Odobel@univ-nantes.fr*

^b*Department of Chemistry, Sapienza University of Rome P. le A. Moro 5, 00185 Rome, Italy*

^c*Institut Universitaire de France, 103 blvd St Michel, 75005 Paris Cedex 5, France. E-mail: Denis.Jacquemin@univ-nantes.fr*

Abstract

In this study, we have investigated for the first time the use of isoindigo derivatives as sensitizers in NiO-based dye-sensitized solar cells (DSSCs). For this purpose, two indigo sensitizers were prepared and their electronic properties were characterized by UV/visible spectroscopy, cyclic voltammetry and time-dependent density functional theory (DT-DFT). The first dye contains a N,N-Di(4-benzoic acid)phenylamine moiety acting as anchoring/donor group, the isoindigo acting as the acceptor, while the second compounds is a dyad which is based on the same structure, but is additionally functionalized with a naphthalene imide unit, acting as secondary electron acceptor. The electronic properties were also modeled by DT-DFT quantum chemistry calculations and they revealed that a charge transfer band is present between the trisarylamine donor part and the isoindigo moiety. The photovoltaic performances of these new dyes were evaluated in NiO-based DSSCs with both iodide/triiodide and cobalt electrolytes. It turned out that they perform well since the photocurrent was generated up to the wavelength of 700 nm. Altogether, these results underscore the viability of isoindigo dyes for *p*-DSSCs.

Introduction

Dye sensitized photocathodes based on *p*-type semiconductors (*p*-SC) are valuable systems for solar energy conversion schemes because they represent the complementary photoelectrodes to be paired with a photoanode (typically, a sensitized TiO₂ film) in order to develop tandem photovoltaic cells and tandem photoelectrocatalytic devices for artificial photosynthesis.¹ A *p*-type dye sensitized

solar cell (*p*-DSSC) is composed of a nanocrystalline film of a wide bandgap *p*-SC (generally NiO) covered by a monolayer of a sensitizer. Light excitation of the sensitizer promotes hole injection into the valence band of the *p*-SC and the reduced sensitizer is subsequently regenerated by a redox mediator.¹⁻² Although a significant amount of work has been undertaken for several years in this field, there are only a relatively small number of dye families that have been investigated with the purpose of obtaining efficient *p*-DSSCs.³ For example, perylene imides,⁴ push-pull systems,⁵ diketopyrrolopyrroles (DPPs),⁶ squaraines,⁷ BODIPYs,⁸ porphyrins,⁹ ruthenium¹⁰ and iridium¹¹ polypyridine complexes were studied in NiO based *p*-DSSCs and some of them proved to be rather effective sensitizers. Nevertheless, the best performing dyes, namely push-pull systems,^{5b, 12} deliver a short current density (J_{sc}) of 8.2 mA/cm²,¹³ a value that remains low compared to those delivered by many sensitizers on TiO₂ based photoanodes ($J_{sc} > 15$ mA/cm²).¹⁴ This motivated us to investigate the performances of indigo derivatives in the framework of *p*-SC. More specifically, we focus here on isoindigo derivatives. Isoindigo is a structural isomer of the famous indigo dye known since the antiquity and still largely used in the industry owing to its intense blue color and very high photostability. Isoindigo is a well-known key building block used in the design of organic materials for molecular electronic applications, especially for organic solar cells and organic field effect transistors.¹⁵ Moreover, isoindigo sensitizers were also successfully implemented in conventional DSSCs based on TiO₂ photoanodes.¹⁶ Recently, we have shown that DPP derivatives are promising sensitizers for *p*-DSSCs⁶ and isoindigo presents a structure closely related to DPP. However, isoindigo was never investigated as potential sensitizer for *p*-DSSCs in spite of its *a priori* suitable photoredox properties. Indeed, isoindigo intensely absorbs in the visible spectrum and is an electron accepting unit like DPP. Therefore, it represents an attractive moiety to engineer efficient sensitizers for *p*-DSSCs. In this study, we have prepared and characterized the photovoltaic performances in *p*-DSSC of two isoindigo dyes, namely **ISO-Br** and **ISO-NDI** (Chart 1). The results support the great potential of these systems for this application.

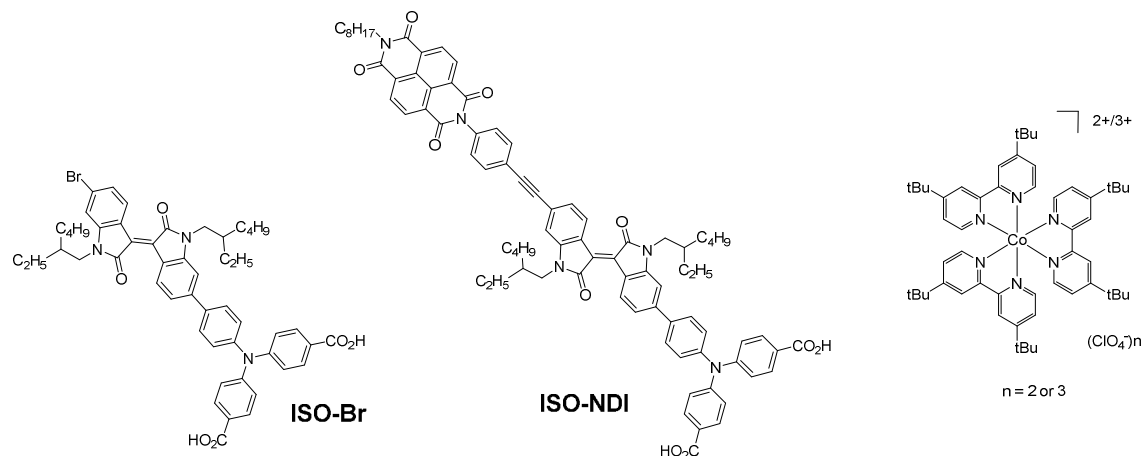


Chart 1. Structures of the isoindigo dyes investigated in this study and of the cobalt complexes used as redox mediator (cobalt electrolyte).

Experimental part

¹H and ¹³C NMR were recorded on a Bruker ARX 300 MHz, AVANCE 300 and 400 Bruker. Chemical shifts for ¹H and ¹³C NMR spectra are referenced to residual protium in the deuterated solvent (CDCl₃ δ = 7.26 ppm for ¹H and δ = 77.16 ppm for ¹³C, CD₃OD δ = 3.31 ppm for ¹H, DMSO d₆ δ = 2.50 ppm for ¹H and δ = 39.52 ppm for ¹³C). Spectra were recorded at room temperature, chemical shifts are

written in ppm and coupling constants in Hz. High-resolution mass spectra (HR-MS) were obtained either by electrospray ionization coupled with high resolution ion trap orbital (LTQ-Orbitrap, ThermoFisher Scientific,) or by MALDI-TOF-TOF (Autoflex III de Bruker), both working in ion positive mode. Electrochemical measurements were made under an argon atmosphere at room temperature in DMF and in presence of 0.1 M Bu_4NPF_6 as supporting electrolyte. Cyclic voltammetry experiments were performed by using an Autolab PGSTAT 302N potentiostat/galvanostat. A standard three-electrode electrochemical cell was used. All potentials are quoted relative to saturated calomel electrode (SCE). The working electrode was platinum (3 mm in diameter) (E_{pa} , anodic peak potential, E_{pc} , cathodic peak potential; $E_{1/2}=(E_{pa} + E_{pc})/2$; $\Delta E_p = E_{pa} - E_{pc}$). The auxiliary electrode was a stainless steel wire. In all the experiments the scan rate was $100 \text{ mV}\cdot\text{s}^{-1}$. UV Visible absorption spectra was recorded on an UV 2501PC Shimadzu spectrophotometer, using 1 cm path length cells. FT-IR spectra were recorded on a Bruker Tensor 27 Fourier Transform spectrometer equipped with a SPECAC Quest ATR diamond accessory.

Chemicals were purchased from Sigma-Aldrich or Alfa Aesar and used as received. Thin-layer chromatography (TLC) was performed on aluminum sheets precoated with Merck 5735 Kieselgel 60F254. Column chromatography was carried out with Merck 5735 Kieselgel 60F (0.040-0.063 mm mesh). The compounds 6,6'-Dibromo-N,N'-(1-ethylhexyl)-isoindigo **1**^{16d}, N,N-Di(4-benzoic acid tert-butyl ester)-4-trimethylsilanylethynyl-phenylboronate ester **2**¹⁷ and N-(4-Ethynyl-phenyl)-N'-(n-octyl)-naphthalene-diimide **4**¹⁸ were prepared according to methods published in the literature. NiO nanoparticles were purchased from Inframat (diameter: 20 nm and surface area: $77 \text{ m}^2/\text{g}$.)

Photovoltaic measurements:

Conductive glass substrates (F-doped SnO_2) were purchased from Solaronix (TEC15, sheet resistance $15 \Omega/\text{square}$). Conductive glass substrates were successively cleaned by sonication in soapy water, then acidified ethanol for 10 min before being fired at $450 \text{ }^\circ\text{C}$ for 30 min. Once cooled down to room temperature, FTO plates were screen printed with NiO using a home-made paste. The NiO screen-printing paste was produced by preparing a slurry of 3 g of NiO nanopowder (Inframat) suspended in 10 mL of distilled ethanol and ball-milled (500 rpm) for 24 h. The resulting slurry was mixed in a round-bottom flask with 10 ml of 10 wt% ethanolic ethyl cellulose (Sigma Aldrich) solution and 20 ml terpineol, followed by slow ethanol removal by rotary evaporation. The dried film was calcined in air at $400 \text{ }^\circ\text{C}$ for 0.5 h. The prepared NiO electrodes ($1.2 \mu\text{m}$ thick) were soaked while still hot ($80 \text{ }^\circ\text{C}$) in a 0.16 mM solution of each dye and were kept dipped for 16 h. A mixture of distilled acetonitrile and tert-butanol was used (1/1, v/v) for each bath.

Electrolytes used are composed of: 1 M lithium iodide and 0.1M diiodine in acetonitrile for I_3^-/I^- electrolyte and 0.1 M $\text{Co}^{\text{II}}(\text{dtb-bpy})_3$, 0.1 M $\text{Co}^{\text{III}}(\text{dtb-bpy})_3$ and 0.1M LiClO_4 in propylene carbonate for cobalt complex as redox shuttle. Platinum counter electrodes were prepared by depositing a few drops of an isopropanol solution of hexachloroplatinic acid in distilled isopropanol (2 mg per mL) on FTO plates (TEC7, Solaronix). Substrates were then fired at 375°C for 30 mn. The photocathode and the counter electrode were placed on top of each other and sealed using a thin transparent film of Surlyn polymer (DuPont, $25 \mu\text{m}$) as spacer. A drop of electrolyte was introduced through a predrilled hole in the counter electrode by vacuum backfilling, the hole was then sealed by a glass stopper with surlyn. The cell had an active area of 0.25 cm^2 .

The current-voltage characteristics were determined by applying an external potential bias to the cell and measuring the photocurrent using a Keithley model 2400 digital source meter. The solar simulator is an Oriel Lamp calibrated to $100 \text{ mW}/\text{cm}^2$.

Synthesis of dye **3**:

To a solution of N,N-Di(4-benzoic acid tert-butyl ester)-4-trimethylsilanylethynyl-phenylboronate ester **2** (52 mg, 0.09 mmol) and 6,6'-Dibromo-N,N'-(2-ethylhexyl)-isoindigo **1** (120 mg, 0.19 mmol) in a mixture of 5 mL of tetrahydrofuran/ water mixture (5/1) were added potassium carbonate (37 mg, 0.27 mmol) and tetrakis(triphenylphosphine)palladium (6 mg, 5.10^{-3} mmol) under nitrogen. The mixture was stirred overnight at 80°C and then poured into water. The organic phase was extracted by CH₂Cl₂, washed with brine and dried over MgSO₄. After removal of the solvent under reduced pressure, the purple solid was purified by column chromatography on silica gel eluted with CH₂Cl₂ to give dye **3** (74 mg, 81%). ¹H-NMR (CD₃OD) δ = 9.28 (d, J = 6 Hz, 1H), 9.16 (d, J = 6 Hz, 1H), 7.91 (d, J = 9 Hz, 4H), 7.77 (d, J = 9 Hz, 2H), 7.32 (d, J = 9 Hz, 1H), 7.24 (d, J = 9 Hz, 2H), 7.15-7.07 (m, 7H), 3.75-3.68 (m, 4H), 1.90 (m, 2H), 1.58 (s, 18H), 1.39-1.27 (m, 16H), 0.95-0.85 (m, 12H). ¹³C-NMR (CDCl₃) δ = 168.7, 168.3, 165.4, 150.5, 147.0, 146.7, 144.4, 136.5, 133.5, 130.6, 130.5, 130.4, 128.2, 126.7, 126.2, 125.9, 125.1, 123.1, 120.6, 111.5, 106.3, 80.9, 53.5, 44.5, 37.8, 37.5, 30.8, 30.3, 29.8, 28.8, 28.7, 28.3, 24.2, 24.1, 23.1, 14.2, 10.9, 10.8. HRMS (MALDI) Calculated for C₆₀H₇₀BrN₃O₆ (M+H)⁺ : 1008.4526, found : m/z 1008.4512.

Synthesis of dye **5**:

To a solution of compound **3** (27 mg, 0.027 mmol) and N-(4-Ethynyl-phenyl)-N'-(n-octyl)-naphthalene-diimide **4** (25 mg, 0.054 mmol) in 4 mL of toluene were added triethylamine (0.5 mL), copper iodide (7 mg, 0.037 mmol) and tetrakis(triphenylphosphine) palladium (10 mg, 0.0086 mmol) under nitrogen. The mixture was stirred overnight at 60°C and then poured into water. The organic phase was extracted by CH₂Cl₂, washed with brine and dried over MgSO₄. After removal of the solvent under reduced pressure, the purple solid was purified by column chromatography on silica gel eluted with CH₂Cl₂ to give dye **5** (8 mg, 21%). ¹H-NMR (CDCl₃) δ = 9.20 (d, J=9 Hz, 1H), 9.15 (d, J = 9 Hz, 1H), 8.80 (s, 4H), 7.89 (d, J = 9 Hz, 4H), 7.76 (d, J = 9 Hz, 2H), 7.58 (d, J = 9 Hz, 2H), 7.34 (d, J = 9 Hz, 2H), 7.24 (m, 4H), 7.14 (d, J = 9 Hz, 4H), 6.94 (d, J = 9 Hz, 2H), 4.20 (t, 9 Hz, 2 H), 3.70 (m, 4H), 1.90 (m, 2H), 1.74 (m, 2H), 1.59 (s, 18H), 1.50-1.20 (m, 26 H), 1.00-0.80 (m, 15 H). ¹³C-NMR (CDCl₃) δ = 168.7, 168.5, 165.4, 163, 162.9, 150.5, 147.0, 146.2, 145.1, 144.4, 136.5, 134.8, 133.5, 133.0, 131.6, 131.2, 131.1, 129.6, 128.9, 128.3, 127.2, 126.7, 126.6, 125.9, 124.1, 123.1, 122.1, 120.9, 120.7, 110.9, 106.3, 91.4, 80.9, 44.5, 41.2, 37.9, 37.7, 31.9, 31.7, 30.9, 30.8, 29.4, 28.9, 28.8, 27.2, 24.2, 23.2, 22.8, 14.2, 10.9, 10.8 HRMS (MALDI) Calculated for C₉₀H₉₅N₅O₁₀ (M+H)⁺ : 1406.7157, found : m/z 1406.7160.

Synthesis of dyes **ISO-Br** and **ISO-NDI**:

To a solution of dye **3** (18 mg, 0.017 mmol) (or dye **5** (8 mg, 0.0057 mmol)) in dichloromethane (2mL), trifluoroacetic acid (2 mL) was added under nitrogen. The mixture was stirred for 2 hours at room temperature. After removal of the solvent under reduced pressure, the product was dried under vacuum to give **ISO-Br** (or **ISO-NDI**) with quantitative yield.

ISO-Br : ¹H-NMR (DMSO) δ = 9.12 (d, J = 6 Hz, 1H), 9.01 (d, J = 6 Hz, 1H), 7.91 (d, J = 9 Hz, 4H), 7.81 (d, J = 9 Hz, 2H), 7.34 (d, J = 9 Hz, 1H), 7.24-7.20 (m, 5H), 7.13 (d, 4H), 3.70-3.60 (m, 4H), 1.84-1.78 (m, 2H), 1.39-1.15 (m, 16H), 0.90-0.75 (m, 12H). FT-IR (ATR) ν_{max} (cm⁻¹): 2956, 2925, 2857, 1681, 1592,

1313, 1263, 1170, 1105, 1072, 814, 770, 699. HRMS (MALDI) calculated for $C_{52}H_{54}BrN_3O_6$ (M+H)⁺ : 896.3274, found : m/z 896.3309.

ISO-NDI : ¹H-NMR (CDCl₃/MeOD) δ = 9.20 (d, J=9 Hz, 1H), 9.15 (d, J = 9 Hz, 1H), 8.78 (s, 4H), 7.95 (d, J = 9 Hz, 4H), 7.75 (d, J = 9 Hz, 2H), 7.59 (d, J = 9 Hz, 2H), 7.32 (d, J = 9 Hz, 2H), 7.25-7.18 (m, 4H), 7.14 (d, J = 9 Hz, 4H), 6.94 (d, J = 9 Hz, 2H), 4.20 (t, 9 Hz, 2 H), 3.70 (m, 4H), 1.90 (m, 2H), 1.74 (m, 2H), 1.50-1.20 (m, 26 H), 1.00-0.80 (m, 15 H). FT-IR (ATR) ν_{max} (cm⁻¹): 2956, 2926, 2857, 1708, 1666, 1593, 1509, 1452, 1340, 1317, 1245, 1171, 1104, 813, 767, 707. HRMS (MALDI) calculated for $C_{82}H_{79}BrN_5O_{10}$ (M+H)⁺ : 1294.5905 found : m/z 1294.5892.

Theoretical simulations

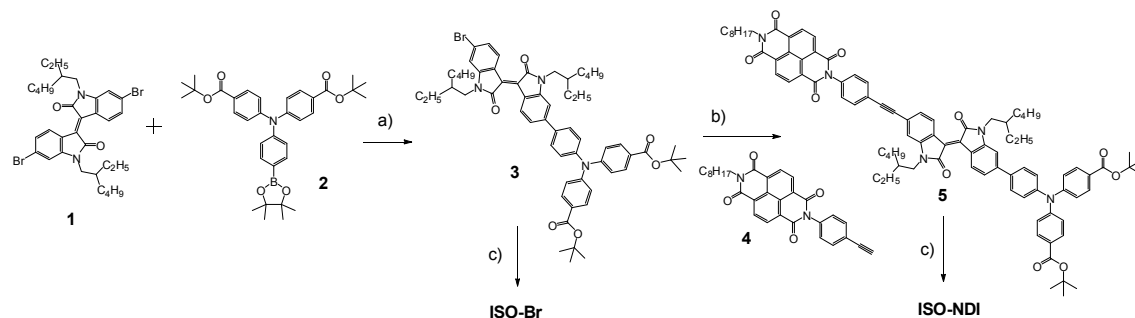
All simulations have been achieved with the Gaussian09 program,¹⁹ using Density Functional Theory (DFT) and Time-Dependent DFT (TD-DFT), for the ground and excited state properties, respectively. The computational protocol proceeds through a four step strategy that is efficient to determine the charge transfer features of rod-like organic dyes: 1) the ground-state geometrical parameters have been determined at the PBE0/6-311G(d,p) level,²⁰ *via* a force-minimization process using a SCF convergence threshold of at least 10⁻⁹ a.u.; 2) the vibrational spectrum of each derivative has been determined analytically at the same level of theory, that is PBE0/6-311G(d,p), and it has been checked that all structures correspond to true minima of the potential energy surface; 3) the first ten low-lying excited-states have been determined within the vertical TD-DFT approximation using the CAM-B3LYP/6-311+G(2d,p)²¹ level of approximation with a tight SCF convergence threshold (at least 10⁻¹⁰ a.u.); 4) the charge-transfer parameters have been estimated with the procedure defined by Le Bahers²² and co-workers using the CAM-B3LYP electronic densities. It proposes to evaluate the distance separating the barycenters of the electron density gain/depletion upon electron transition. All calculations systematically include a modelling of bulk solvent effects (here dimethylformamide) through the Polarizable Continuum Model (PCM).²³ During the simulations, the long alkyl chains attached to the isoindigo moiety have been replaced by methyl groups in order to lighten the computational burden.

Results and discussion

Synthesis of the dyes

The isoindigo chromophore was functionalized by a N,N-Di(4-benzoic acid)phenylamine as this electron rich moiety is well-suited, on the one hand to assist hole injection into NiO valence band and on the other hand to enable a strong grafting of the dye onto NiO surface thanks to the presence of two carboxylic acid groups.^{5,7b,8b} The functionalization of isoindigo unit was made in 6,6' positions because this substitution pattern gives a higher conjugation degree than in 5,5' and therefore enhances the charge transfer transition with the nearby electron donating substituent.^{15a} Branched alkyl chains on lactame moiety promote good solubility of the dye and limit aggregation upon immobilization on NiO surface.^{16d} The naphthalene diimide (NDI) group was introduced to slow down charge recombination between the reduced dye and the injected hole. Indeed, we and others have extensively observed that the latter reaction is particularly fast on NiO and that the introduction of this secondary electron acceptor can dramatically enhance the lifetime of the charge separated state.^{1a, 2, 4b} The syntheses of these two new dyes are described in Scheme 1 and employ the known 6,6'-Dibromo-N,N'-(1-ethylhexyl)-isoindigo **1** as starting material.^{16d} Dibromo isoindigo **1** was coupled

to the anchoring N,N-Di(4-benzoic acid tert-butyl ester)-4-trimethylsilanylethynyl-phenylboronate ester **2** via a Suzuki cross-coupling reaction to give dye **3** with 81% yield after purification. The naphthalene diimide (NDI) moiety was grafted on **3** by a Sonogashira reaction with the N-(4-Ethynyl-phenyl)-N'-(n-octyl)-naphthalene-diimide **4** to lead to dye **5** with a 21% yield. Finally, the *tert*-butyl ester groups in dyes **3** and **5** were hydrolyzed by TFA in an almost quantitative yield to furnish the dyes **ISO-Br** and **ISO-NDI**.



Scheme 1. Synthetic route to **ISO-Br** and **ISO-NDI**. Reagents and conditions: a) K_2CO_3 , $Pd(PPh_3)_4$, THF- H_2O 5:1, overnight, $85^\circ C$; b) CuI , $Pd(PPh_3)_4$, Toluene, NEt_3 , overnight, $60^\circ C$; c) TFA, CH_2Cl_2 , 2 hours, rt.

Electronic absorption spectra

The absorption spectra of the dyes **ISO-Br** and **ISO-NDI** recorded in DMF solution and on mesoporous thin NiO film are shown in Figure 1 and the data are collected in Table 1.

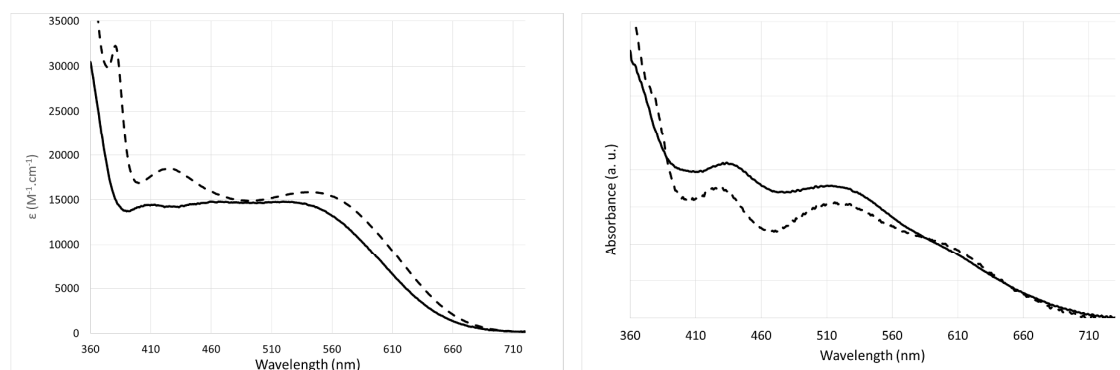


Figure 1. Absorption spectra of the dyes **ISO-Br** (straight line) and **ISO-NDI** (dashed line) recorded in DMF solution (left) and on 600 nm mesoporous thin NiO film (right).

The spectra of the dyes in solution feature a first intense absorption band localized in the UV region, which is assigned to $\pi-\pi^*$ aromatic transitions localized on isoindigo or NDI moieties and a second broad band between 400-600 nm which tails until 700 nm. The latter corresponds to an intramolecular charge transfer transition between the arylamine donor and the isoindigo acceptor moiety (see DFT calculations below). The molar absorption coefficient of the charge transfer transition is around $1.5 \times 10^4 \text{ M}^{-1} \text{ cm}^{-1}$, which is a significant value, but lower than the best performing p-DSSC sensitizers.^{5b, 5c} On mesoporous NiO films, the absorption spectra of the dyes are red shifted relative to those recorded in DMF solution, meaning that after binding on the surface there is either

a little induced aggregation of J-type or there is weak perturbation of the electronic properties of the dyes upon attachment of the acid group to the NiO surface.

Table 1. Maximum absorption wavelength (λ_{abs}) with extinction coefficient (ϵ) recorded at room temperature in DMF solution.

Dyes	$\lambda_{\text{abs}}/\text{nm}$ ($\epsilon/\text{M}^{-1}\text{cm}^{-1}$)
ISO-Br	520 (1.48×10^4); 460 (1.50×10^4); 410 (1.44×10^4)
ISO-NDI	544 (1.59×10^4); 425 (1.85×10^4)

Electrochemical study

The redox potentials of the dyes were recorded in solution to estimate the driving forces for the hole injection reaction from the excited-state into the valence band of NiO and for regeneration reaction with the redox mediator [$\text{I}_3^- + \text{dye}^- \rightarrow \text{dye} + \text{I}_2^\bullet$ or $\text{Co(III)} + \text{dye}^- \rightarrow \text{dye} + \text{Co(II)}$]; the data are collected in Table 2. The first oxidation in both **ISO-Br** and **ISO-NDI** is a process essentially centered on the arylamine moiety (at ca. 0.95V), because the oxidation of dibromo isoindigo **1** is more positive than 1.5 V (the upper limit of the electrochemical window in DMF in our conditions). This result is in agreement with the quantum calculations (see below) which indicate that the HOMO is centered on the arylamine moiety (Figure 3). This also confirms that isoindigo is rather an electron deficient dye as its reduction is more accessible. Indeed, the dibromo isoindigo **1** is reversibly reduced at -0.79 V, while first reduction in both **ISO-Br** and **ISO-NDI** takes place at a more cathodic potential (at ca. -0.90 V), reflecting the electron releasing property of the trisarylamine, which destabilizes the radical anion (Table 2). The first NDI centered reduction in **ISO-NDI** occurs at -0.65 V, indicating that there is a significant driving force ($\Delta G = -0.28$ eV) for the electron shift reaction ('ISO-NDI \rightarrow ISO-NDI') to occur.

These isoindigo dyes are non luminescent and the 0-0 transition energy (E_{00}) was estimated from the wavelength at the foot of the lowest energy absorption band ($E_{00} = 1.75$ eV). These data were used to build a diagram showing the Gibbs free energy of each charge separation step according to the dye and the redox mediator involved (Figure 2). The calculations indicate that these dyes display significantly exergonic reaction of injection (at ca. -0.5 eV) and very large regeneration driving force especially with cobalt electrolyte. In conclusion, from the thermodynamic point of view, these dyes fulfill the energetic criteria to be efficient NiO sensitizers with both iodide/triiodide and cobalt electrolytes.

Table 2. Redox potentials recorded at room temperature in DMF solution with Bu_4NPF_6 (0.15 M) as supporting electrolyte and referenced *versus* saturated calomel electrode (SCE).

Dyes	$E_{\text{Red}}(\text{ISO}/\text{ISO}^-)$ V	$E_{\text{Red}}(\text{ISO}^+/\text{ISO})$ V	$E_{\text{Red}}(\text{NDI}/\text{NDI}^-)$ V	$^a E_{\text{Red}}(\text{ISO}^*/\text{ISO}^-)$ V	$^b \Delta G_{\text{inj}}$ eV	$^c \Delta G_{\text{reg}}$ with I_3^- eV	$^d \Delta G_{\text{reg}}$ with Co^{III} eV
1	-0.79	> 1.5 V	-				
ISO-Br	-0.90	0.95	-	0.85	-0.55	-0.58	-1.11
ISO-NDI	-0.93	0.94	-0.65	0.82	-0.52	-0.33	-0.86

^aCalculated according to the equation: $E_{\text{Red}}(\text{ISO}^*/\text{ISO}^-) = E_{\text{Red}}(\text{ISO}/\text{ISO}^-) + E_{00}$. ^bCalculated according to the equation: $\Delta G_{\text{inj}} = E_{\text{Red}}(\text{ISO}^*/\text{ISO}^-) - E_{\text{VB}}(\text{NiO})$ with $E_{\text{VB}}(\text{NiO})$ corresponding to the valence band potential of NiO taken as 0.3 V vs SCE.²⁴ ^cCalculated according to the equation: $\Delta G_{\text{reg}} = E_{\text{Red}}(\text{ISO}/\text{ISO}^-) - E(\text{I}_3^-/\text{I}_2^{\bullet-})$ with $E(\text{I}_3^-/\text{I}_2^{\bullet-}) = -0.32$ V. ^dCalculated according to the equation: $\Delta G_{\text{reg}} = E_{\text{Red}}(\text{ISO}/\text{ISO}^-) - E(\text{Co}^{\text{III}}/\text{Co}^{\text{II}})$ with $E(\text{Co}^{\text{III}}/\text{Co}^{\text{II}}) = 0.21$ V.²⁵

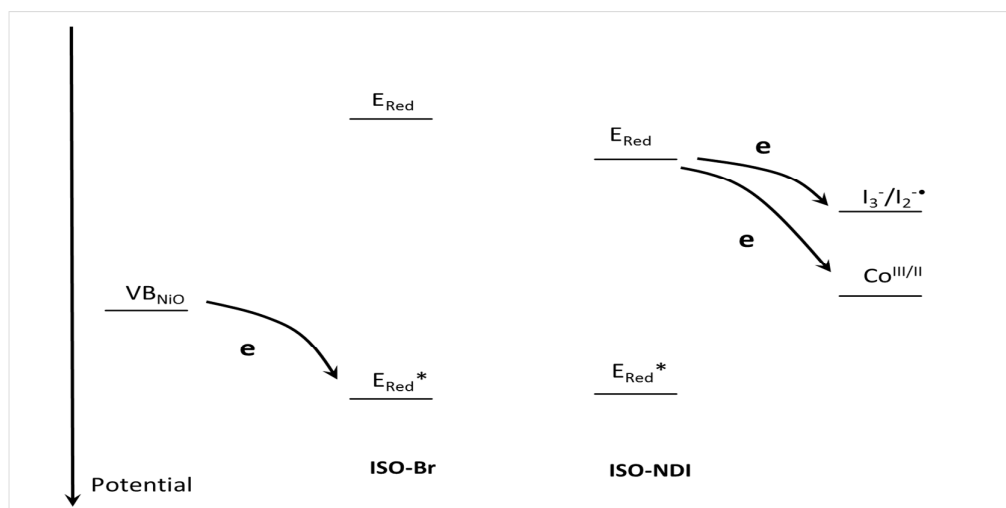


Figure 2. Energy diagram of the relevant levels for the hole photoinjection and dye regeneration reactions in the NiO based p-DSSC.

Quantum chemical calculations

The electronic properties were also investigated by density functional theory (TD-DFT) calculations. For **ISO-Br**, TD-DFT foresees a first transition at 487 nm. This electronic excitation is very intense (f , the associated oscillator strength is 0.69) and corresponds to a blend of HOMO-1 to LUMO and HOMO to LUMO orbital transitions (Figure 3). It is clear that the LUMO is mainly centered on the

isoindigo moiety, whereas the HOMO is largely located on the trisarylamine fragment. In order to obtain a single-figure representation of the impact of the electronic effect, the density difference plots for **ISO-Br** is plotted in Figure 4. It turns out that the amine group acts as a donor (mostly in blue) towards the isoindigo moiety, but the transition is mainly localized on the isoindigo dye.

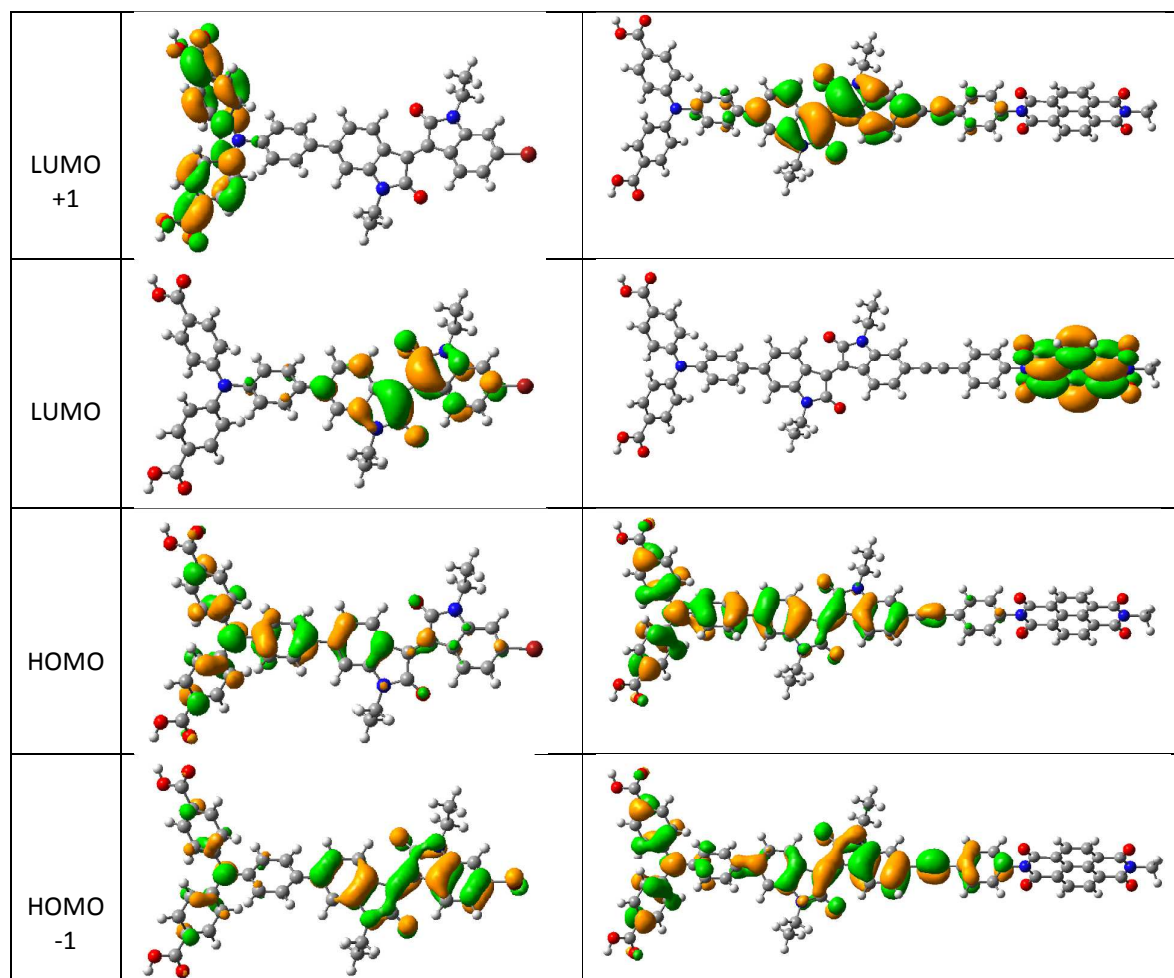


Figure 3. Representation of the frontier molecular orbitals for **ISO-Br** (left) and **ISO-NDI** (right).

We have computed a charge-transfer of $0.56 e$ on a 2.03 \AA distance, the electron going in the expected directions for suitable hole injection in a p-SC. Compared to previous works, such charge-transfer can be considered as significant without being particularly large.¹¹ For **ISO-NDI**, the first transition appears at slightly longer wavelength (508 nm , $f=1.15$) owing to electron delocalization on the ethynyl link (Figure 4). The visible transition mainly corresponds to a blend of HOMO-1 to LUMO+1 and HOMO to LUMO+1 orbital transitions (Figure 3). It is clear that the LUMO+1 is mainly centered on the isoindigo moiety whereas the two occupied orbitals are more delocalized than in **ISO-Br**. The LUMO is not involved in this transition, but is clearly localized on the NDI moiety, which is electronically decoupled to the isoindigo unit. This confirms that NDI is an effective secondary acceptor with respect to the isoindigo, in agreement with the reduction potentials of these units. The density difference plots for **ISO-NDI** is also shown in Figure 4. Again, it is rather similar to the one of **ISO-Br**, but with a perceptible delocalization on the ethynyl group. However, the computed charge-

transfer distance is 1.15 Å, indicating that the initial electron-hole separation is significantly less efficient than in **ISO-Br**.

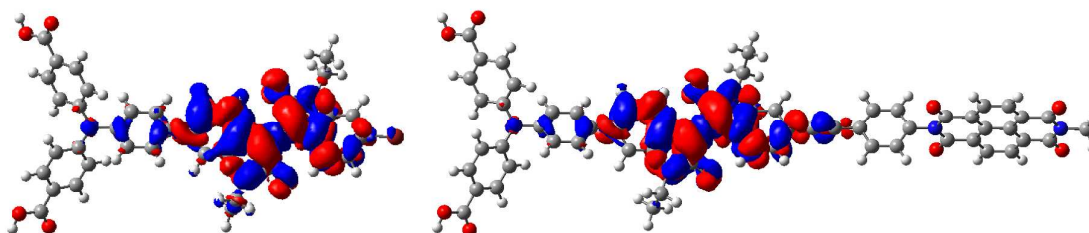


Figure 4. Density difference plots for the first excited-state of **ISO-Br** (left) and **ISO-NDI** (right). The red (blue) regions represent increase (decrease) of electron density upon photon absorption. The selected contour threshold is 4.10^{-4} a.u.

Dye loading determination

To quantify the dye loading on the monocrystalline films of DSSCs, desorption experiments are generally carried out using a base (usually NaOH or Bu_4NOH in DMF). However, these indigo dyes are unstable in basic conditions, probably owing to nucleophilic attack of the hydroxyl ions on the lactam ring of the isoindigo moiety. Accordingly, we have developed another strategy based on the competitive adsorption of an adsorbent which has a stronger affinity to NiO surface than the carboxylic acids. For this purpose, we have selected phenyl-phosphonic acid because: 1) it is an acid, therefore it is harmless for the dyes; 2) it is a colorless compound therefore it does not interfere with indigo absorption in the visible region and 3) phosphonic acids are known to bind more strongly to most metal than carboxylic acid group. Towards this goal, the absorption spectra for various concentrations of **ISO-Br** and **ISO-NDI** in DMF solutions containing phenylphosphonic acid (50 mg.ml^{-1}) were recorded (Figure 5). The absorbance at 520 nm (**ISO-Br**) and 540 nm (**ISO-NDI**) are indeed proportional to the concentration of the dye and enables to safely to determine the extinction coefficient of **ISO-Br** 520 nm ($\epsilon = 1.48 \times 10^4 \text{ M}^{-1}\text{cm}^{-1}$) and that of **ISO-NDI** at 540 nm ($\epsilon = 1.70 \times 10^4 \text{ M}^{-1}\text{cm}^{-1}$) in these conditions (Figure 5). Next, photocathodes, coated with **ISO-Br** and **ISO-NDI**, were dipped in a DMF solution containing phenylphosphonic acid (2 ml, 50 mg.ml^{-1}). After about one minute, the color of the NiO film vanished and the solution turned red indicative of the desorption of the dyes. Finally, the quantity of the dye was estimated from the absorbance of the solution. The dye loading on NiO corresponds to $4.03 \times 10^{-8} \text{ mol.cm}^{-2}$ and $1.11 \times 10^{-8} \text{ mol.cm}^{-2}$ for **ISO-Br** and **ISO-NDI** respectively. Interestingly, we can notice that the dye loading of the bulky **ISO-NDI** is about four times lower than that of **ISO-Br**, which can be explained by its larger molecular footprint, in lines with similar results with very bulky dyes.²⁶ These values are in the range of those reported with dyes anchored with the same N,N-Di(4-benzoic acid)phenylamine (around $1 \times 10^{-8} \text{ mol.cm}^{-2}$)²⁷ but lower than that of the famous P1 dye anchored with a single carboxylic acid group ($12.3 \times 10^{-8} \text{ mol.cm}^{-2}$)²⁸ and the highly performing push-pull thienoquinoidal dye recently reported ($8.5 \times 10^{-8} \text{ mol.cm}^{-2}$).¹³

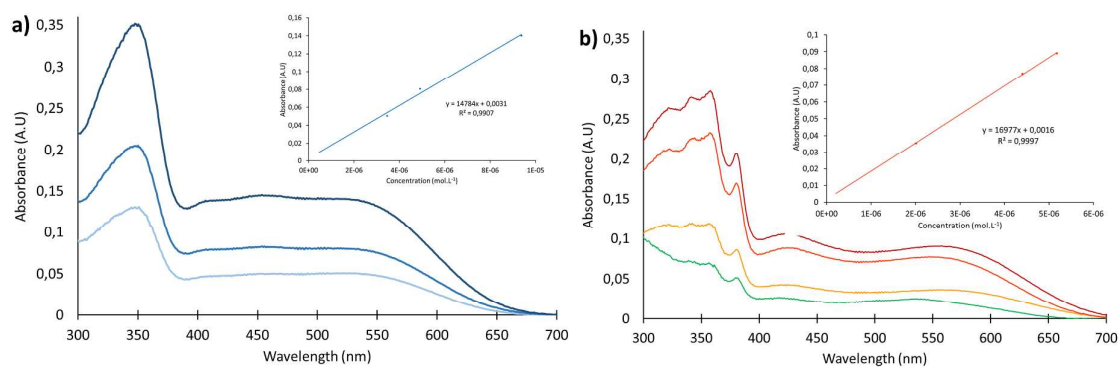


Figure 5. Absorption spectra of **ISO-Br** (a) and **ISO-NDI** (b) at various concentrations recorded in DMF in presence of phenylphosphonic acid at $50 \text{ mg}\cdot\text{ml}^{-1}$. Inset: linear fit of the absorbance for **ISO-Br** samples at 520 nm (a) and of **ISO-NDI** at 540 nm (b).

Photovoltaic properties

The two new dyes **ISO-Br** and **ISO-NDI** were tested in sandwich dye sensitized solar cell consisting of $1.2 \mu\text{m}$ thick NiO mesoporous film photocathodes with a platinum based counter electrode. Two different redox mediators were investigated: first the classical iodide/triiodide and second the tris(4,4'-ditert-butyl-2,2'-bipyridine)cobalt(III/II) complexes (for compositions see the Experimental Section) and the photovoltaic performances were evaluated under AM 1.5 calibrated artificial sunlight. The photovoltaic characteristics (V_{oc} , J_{sc} , ff and PCE) of the solar cells are listed in Table 3 and the photoaction spectra are shown in Figure 6.

First, independently of the electrolyte composition, the dyad **ISO-NDI** performs better than the simple **ISO-Br**, since both the short circuit photocurrent (J_{sc}) and the open circuit voltage (V_{oc}) are larger than those of **ISO-Br** (Table 3). This conclusion is even more pronounced if we take into account that the dye loading of **ISO-NDI** is four times lower than that of **ISO-Br**. The higher performances of **ISO-NDI** can certainly be explained by the longer-lived charge separated state (h^+ in NiO/ e^- on NDI), owing to the longer distance between the hole and the electron (on NDI rather than on isoindigo). In the dyad **ISO-NDI**, there is a sufficient driving force for the electron that moves from the reduced Isoindigo unit to the NDI thus leading ultimately to a longer distance between the hole in NiO and the electron on the NDI. This new charge separated state is longer-lived than that with **ISO-Br**. It is well accepted that charge recombination is the major source of losses in p-DSSCs (see introduction). Therefore, decreasing the rate of this reaction directly impacts the photovoltaic performances of the resulting solar cells. With the iodide electrolyte, a significant part of the photocurrent is produced below 400 nm, which is certainly due to the photoactivity of triiodide anion (direct hole injection in NiO from I_3^{*-}).²⁹ Interestingly, the simple sensitizer **ISO-Br** is particularly active with the cobalt electrolyte, which is known to be only compatible with long-lived charge separated states.^{4a, 4b, 25} Usually, simple dyes or those giving short-lived charge separated state are not compatible with such cobalt electrolyte because Co(III) is a slow electron acceptor (microsecond time scale).^{2, 4a, 8b} The fact that **ISO-Br** exhibits similar values of J_{sc} with both electrolytes and taking into account that cobalt electrolyte itself cannot produce photocurrent, implies that the charge separated state of this dye is probably significantly long-lived albeit shorter than in **ISO-NDI**. This is consistent with the localization of the LUMO orbital mainly on the isoindigo moiety, without significant extension of the anchoring group (Figure 3). Furthermore, these indigo dyes are active even at quite long wavelengths since their IPCE spectra extend up to 700 nm (Figure 6).

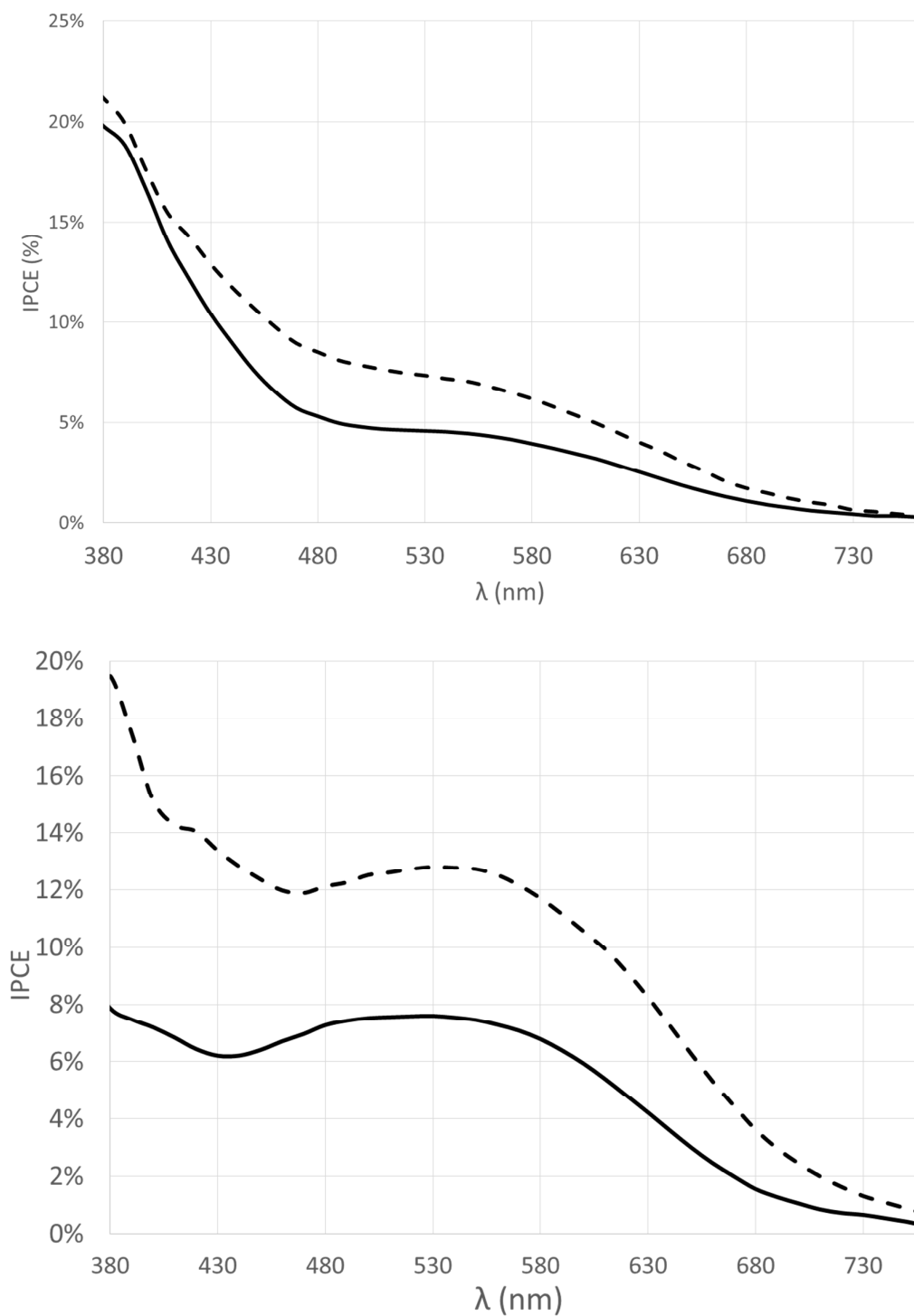


Figure 6. IPCE spectra of NiO-based p-DSSCs sensitized with the isoindigo dyes **ISO-Br** (straight line) and **ISO-NDI** (dashed line) with iodide/triiodide electrolyte (up) and cobalt electrolyte (down).

Table 3. Photoelectrochemical characteristics of the p-DSCs with DPP sensitizers employing either the iodide/triiodide or cobalt electrolytes recorded under AM1.5 G simulated sunlight (1000 W/m²).

Dye	electrolyte	Jsc mA/cm ²	Voc mV	ff %	PCE %
ISO-Br	I ₃ ⁻ /I ⁻	0.82	87	34	0.025
	Co ^{III/II}	0.80	182	23	0.033
ISO-NDI	I ₃ ⁻ /I ⁻	1.27	96	33	0.040
	Co ^{III/II}	1.54	260	25	0.100

Overall, these results indicate that isoindigos are active sensitizers in NiO based *p*-DSSC. If we consider the low thickness of the NiO films employed herein and the moderate extinction coefficient of the visible absorption band of isoindigo, the photovoltaic performances of these new sensitizers are particularly significant which augurs well for the use of this class of dye in *p*-DSSCs.

Conclusions

In this work we have prepared the first isoindigo sensitizers for *p*-DSSC. These new dyes are characterized by a broad charge transfer band and significant Gibbs free energies for hole injection and dye regeneration with both iodide and cobalt electrolytes. Interestingly, the **ISO-Br** dye is compatible with the cobalt electrolyte, suggesting the formation of a significantly long-lived charge separated state on NiO, which is unusual for a simple system having no secondary acceptor unit. Overall, this study demonstrates the suitability of isoindigo dyes to sensitize NiO. Owing to the simplicity of the structures prepared herein, there is plenty of room for improvement and we can optimistically foresee that further molecular engineering will enhance the photovoltaic performances of the proposed dyes. For example, the introduction of stronger electron donating unit around the isoindigo skeleton should enlarge the intensity of the charge transfer band and shift it to lower energy.

Acknowledgements

ANR is acknowledged for the financial support of these researches through the program POSITIF (ANR-12-PRGE-0016-01) and Région des Pays de la Loire and Nantes University for the project LUMOMAT. D. J. acknowledges both the European Research Council (ERC) and the Région des Pays de la Loire for financial support in the framework of a Starting Grant (Marches – 278845) and a recrutement sur poste stratégique, respectively. This research used resources of (1) the GENCI-CINES/IDRIS (Grant c2014085117) and (2) CCIPL (Centre de Calcul Intensif des Pays de Loire). Aurélien Planchat is acknowledged for the fabrication and the photovoltaic measurements (J/V characteristics and IPCE spectra) while Nadine Szuwarski is acknowledged for the screen printing of the NiO films on FTO substrates.

References

1. (a) F. Odobel, L. Le Pleux, Y. Pellegrin and E. Blart, *Acc. Chem. Res.*, 2010, **43**, 1063-1071; (b) F. Odobel and Y. Pellegrin, *J. Phys. Chem. Lett.*, 2013, **4**, 2551-2564; (c) J. He, H. Lindström, A. Hagfeldt, S.E. Lindquist, *Solar Energy Mater. Solar Cells*, 2010, **62**, 265-273.
2. F. Odobel, Y. Pellegrin, E. A. Gibson, A. Hagfeldt, A. L. Smeigh and L. Hammarström, *Coord. Chem. Rev.*, 2012, **256**, 2414-2423.
3. F. Odobel, Y. Pellegrin, F. B. Anne and D. Jacquemin, in *High-Efficiency Solar Cells - Physics, Materials and Devices*, ed. Z. M. W. a. X. Wang, Springer, 2013.
4. (a) E. A. Gibson, A. L. Smeigh, L. Le Pleux, J. Fortage, G. Boschloo, E. Blart, Y. Pellegrin, F. Odobel, A. Hagfeldt and L. Hammarström, *Angew. Chem., Int. Ed.*, 2009, **48**, 4402-4405; (b) A. Morandeira, J. Fortage, T. Edvinsson, L. Le Pleux, E. Blart, G. Boschloo, A. Hagfeldt, L. Hammarström and F. Odobel, *J. Phys. Chem. C*, 2008, **112**, 1721-1728; (c) L. Le Pleux, A. L. Smeigh, E. Gibson, Y. Pellegrin, E. Blart, G. Boschloo, A. Hagfeldt, L. Hammarstrom and F. Odobel, *Energy Environ. Sci.*, 2011, **4**, 2075-2084.
5. (a) M. Weideler, S. Powar, H. Kast, Z. Yu, P. P. Boix, C. Li, K. Müllen, T. Geiger, S. Kuster, F. Nüesch, U. Bach, A. Mishra and P. Bäuerle, *Chem. – Asian J.*, 2014, **9**, 3251-3263; (b) A. Nattestad, A. J. Mozer, M. K. R. Fischer, Y. B. Cheng, A. Mishra, P. Baeuerle and U. Bach, *Nat. Mater.*, 2010, **9**, 31-35; (c) P. Qin, H. Zhu, T. Edvinsson, G. Boschloo, A. Hagfeldt and L. Sun, *J. Am. Chem. Soc.*, 2008, **130**, 8570-8571.
6. L. Favereau, J. Warnan, Y. Pellegrin, E. Blart, M. Boujtita, D. Jacquemin and F. Odobel, *Chem. Commun.*, 2013, **49**, 8018-8020.
7. (a) J. Warnan, J. Gardner, L. Le Pleux, J. Petersson, Y. Pellegrin, E. Blart, L. Hammarström and F. Odobel, *J. Phys. Chem. C*, 2013, **118**, 103-113; (b) C.-H. Chang, Y.-C. Chen, C.-Y. Hsu, H.-H. Chou and J. T. Lin, *Org. Lett.*, 2012, **14**, 4726-4729; (c) G. Naponiello, I. Venditti, V. Zardetto, D. Saccone, A. Di Carlo, I. Fratoddi, C. Barolo, D. Dini, *Appl. Surf. Sci.*, 2015, 356, 911-920.
8. (a) C. J. Wood, G. H. Summers and E. A. Gibson, *Chem. Commun.*, 2015; (b) J.-F. Lefebvre, X.-Z. Sun, J. A. Calladine, M. W. George and E. A. Gibson, *Chem. Commun.*, 2014, **50**, 5258-5260.
9. (a) M. Borgström, E. Blart, G. Boschloo, E. Mukhtar, A. Hagfeldt, L. Hammarström and F. Odobel, *J. Phys. Chem. B*, 2005, **109**, 22928-22934; (b) H. Tian, J. Oscarsson, E. Gabrielsson, S. K. Eriksson, R. Lindblad, B. Xu, Y. Hao, G. Boschloo, E. M. J. Johansson, J. M. Gardner, A. Hagfeldt, H. Rensmo and L. Sun, *Sci. Rep.*, 2014, **4**; (c) A. Maufroy, L. Favereau, F. B. Anne, Y. Pellegrin, E. Blart, M. Hissler, D. Jacquemin and F. Odobel, *J. Mater. Chem. A*, 2015, **3**, 3908-3917.
10. (a) C. J. Wood, K. C. D. Robson, P. I. P. Elliott, C. P. Berlinguette and E. A. Gibson, *RSC Advances*, 2014, **4**, 5782-5791; (b) Z. Ji, G. Natu and Y. Wu, *ACS Appl. Mater. Interfaces*, 2013, **5**, 8641-8648; (c) Z. Ji, G. Natu, Z. Huang, O. Kokhan, X. Zhang and Y. Wu, *J. Phys. Chem. C*, 2012, **116**, 16854-16863.
11. M. Gennari, F. Légalité, L. Zhang, Y. Pellegrin, E. Blart, J. Fortage, A. M. Brown, A. Deronzier, M.-N. Collomb, M. Boujtita, D. Jacquemin, L. Hammarström and F. Odobel, *J. Phys. Chem. Lett.*, 2014, **5**, 2254-2258.
12. L. Li, E. A. Gibson, P. Qin, G. Boschloo, M. Gorlov, A. Hagfeldt and L. Sun, *Adv. Mater.*, 2010, **22**, 1759-1762.
13. Q.-Q. Zhang, K.-J. Jiang, J.-H. Huang, C.-W. Zhao, L.-P. Zhang, X.-P. Cui, M.-J. Su, L.-M. Yang, Y.-L. Song and X.-Q. Zhou, *J. Mater. Chem. A*, 2015.
14. (a) A. Hagfeldt, G. Boschloo, L. Sun, L. Kloo and H. Pettersson, *Chem. Rev.*, 2010, **110**, 6595-6663; (b) A. Mishra, M. K. R. Fischer and P. Bäuerle, *Angew. Chem., Int. Ed.*, 2009, **48**, 2474-2499.
15. (a) R. Stalder, J. Mei, K. R. Graham, L. A. Estrada and J. R. Reynolds, *Chem. Mater.*, 2014, **26**, 664-678; (b) T. Lei, J.-Y. Wang and J. Pei, *Acc. Chem. Res.*, 2014, **47**, 1117-1126; (c) E. Wang, W. Mammo and M. R. Andersson, *Adv. Mater.*, 2014, **26**, 1801-1826.
16. (a) M. Hosseinnazhad, S. Moradian and K. Gharanjig, *Synth. Commun.*, 2014, **44**, 779-787; (b) D. Y. Kwon, D. M. Chang and Y. S. Kim, *Mater. Res. Bull.*, 2014, **58**, 93-96; (c) W. Ying, F. Guo, J. Li, Q. Zhang, W. Wu, H. Tian and J. Hua, *ACS Appl. Mater. Interfaces*, 2012, **4**, 4215-4224; (d) S.-G. Li, K.-J.

- Jiang, J.-H. Huang, L.-M. Yang and Y.-L. Song, *Chem. Commun.*, 2014, **50**, 4309-4311; (e) D. Wang, W. Ying, X. Zhang, Y. Hu, W. Wu and J. Hua, *Dyes Pigm.*, 2015, **112**, 327-334; (f) R. Stalder, D. Xie, A. Islam, L. Han, J. R. Reynolds and K. S. Schanze, *ACS Appl. Mater. Interfaces*, 2014, **6**, 8715-8722; (g) W. Gang, T. Haijun, Z. Yiping, W. Yingying, H. Zhubin, Y. Guipeng and P. Chunyue, *Synthetic Metals*, 2014, **187**, 17-23.
17. M. Weideler, A. Mishra, A. Nattestad, S. Powar, A. J. Mozer, E. Mena-Osteritz, Y.-B. Cheng, U. Bach and P. Bäuerle, *J. Mater. Chem.*, 2012, **22**, 7366-7379.
18. F. Chaignon, M. Falkenström, S. Karlsson, E. Blart, F. Odobel and L. Hammarström, *Chem. Commun.*, 2007, 64-66.
20. C. Adamo and V. Barone, *J. Chem. Phys.*, 1999, **110**, 6158-6170.
21. T. Yanai, D. P. Tew and N. C. Handy, *Chem. Phys. Lett.*, 2004, **393**, 51-57.
19. Frisch MJ, Trucks GW, Schlegel HB, Scuseria GE, Robb MA, Cheeseman JR, Scalmani G, Barone V, Mennucci B, Petersson GA, Nakatsuji H, Caricato M, Li X, Hratchian HP, Izmaylov AF, Bloino J, Zheng G, Sonnenberg JL, Hada M, Ehara M, Toyota K, Fukuda R, Hasegawa J, Ishida M, Nakajima T, Honda Y, Kitao O, Nakai H, Vreven T, Jr, Peralta JE, Ogliaro F, Bearpark M, Heyd JJ, Brothers E, Kudin KN, Staroverov VN, Kobayashi R, Normand J, Raghavachari K, Rendell A, Burant JC, Iyengar SS, Tomasi J, Cossi M, Rega N, Millam JM, Klene M, Knox JE, Cross JB, Bakken V, Adamo C, Jaramillo J, Gomperts R, Stratmann RE, Yazyev O, Austin AJ, Cammi R, Pomelli C, Ochterski JW, Martin RL, Morokuma K, Zakrzewski VG, Voth GA, Salvador P, Dannenberg JJ, Dapprich S, Daniels AD, Farkas, Foresman JB, Ortiz JV, Cioslowski J, Fox DJ, *Gaussian 09 Revision D.01*. Gaussian Inc. Wallingford CT 2009: 2009.
20. C. Adamo and V. Barone, *J. Chem. Phys.*, 1999, **110**, 6158-6170.
21. T. Yanai, D. P. Tew and N. C. Handy, *Chem. Phys. Lett.*, 2004, **393**, 51-57.
22. (a) D. Jacquemin, T. L. Bahers, C. Adamo and I. Ciofini, *Phys. Chem. Chem. Phys.*, 2012, **14**, 5383-5388 Code available at the University of Nantes: <http://www.sciences.univ-nantes.fr/CEISAM/erc/marches/?cat=39>; (b) T. Le Bahers, C. Adamo and I. Ciofini, *J. Chem. Theory Comput.*, 2011, **7**, 2498-2506.
23. J. Tomasi, B. Mennucci and R. Cammi, *Chem. Rev.*, 2005, **105**, 2999-3094.
24. J. He, H. Lindström, A. Hagfeldt and S.-E. Lindquist, *J. Phys. Chem. B*, 1999, **103**, 8940-8943.
25. E. A. Gibson, A. L. Smeigh, L. Le Pleux, L. Hammarström, F. Odobel, G. Boschloo and A. Hagfeldt, *J. Phys. Chem. C* 2011, **115**, 9772-9779.
26. K. A. Click, D. R. Beauchamp, B. R. Garrett, Z. Huang, C. M. Hadad and Y. Wu, *Phys. Chem. Chem. Phys.*, 2014, **16**, 26103-26111.
27. Z. Liu, W. Li, S. Topa, X. Xu, X. Zeng, Z. Zhao, M. Wang, W. Chen, F. Wang, Y.-B. Cheng and H. He, *ACS Appl. Mater. Interfaces*, 2014, **6**, 10614-10622.
28. Y.-S. Yen, W.-T. Chen, C.-Y. Hsu, H.-H. Chou, J. T. Lin and M.-C. P. Yeh, *Org. Lett.*, 2011, **13**, 4930-4933.
29. (a) H. Zhu, A. Hagfeldt and G. Boschloo, *J. Phys. Chem. C*, 2007, **111**, 17455-17458; (b) E. A. Gibson, L. Le Pleux, J. Fortage, Y. Pellegrin, E. Blart, F. Odobel, A. Hagfeldt and G. Boschloo, *Langmuir*, 2012, **28**, 6485-6493.

Graphical abstract for entry

Isoindigo Derivatives for Application in *p*-Type Dye Sensitized Solar Cells

Dorine Ameline, Stéphane Diring, Yoann Farre, Yann Pellegrin, Gaia Naponiello, Errol Blart, Benoît Charrier, Danilo Dini, Denis Jacquemin,* Fabrice Odobel*

